

The Origin of the Stellar Initial Mass Function

Robert Blum, Knut Olsen, and Stephen Strom

National Optical Astronomy Observatory
and
AURA New Initiatives Office

DRAFT
April 28 , 2003

Introduction

The large majority of stars comprising galaxies are believed to form in rich clusters containing between 10^4 and 10^6 stars confined within volumes of 3 to 30 pc^3 . Such clusters are expected to be the most prominent features in pre-galactic clumps and newly-forming galaxies. Their massive stars are the primary source of heavy elements injected into both the interstellar medium of their host systems and the nearby intergalactic medium. Understanding the kinds of stars that form in these regions and what processes control their formation represents an essential first step in understanding the star formation history of galaxies.

Of primary interest to the evolution of galaxies and the intergalactic medium is quantifying the distribution of stellar masses, $N(M)$ in these systems. The shape of $N(M)$ among stars more massive than 5 M_{sun} will control the total quantity and relative abundances of heavy elements enriching the galactic ISM and intergalactic IGM. The ratio of high mass ($M \gg 5 M_{\text{sun}}$) to low mass stars ($M \ll 1 M_{\text{sun}}$) provides a measure of the amount of material available for ‘recycling’ into subsequent generations of stars compared to that contained in stars with lifetimes well in excess of 20 Gyr.

Of equal interest is gaining an understanding of the star formation process in these rich, dense clusters. Recent theoretical work (Elmegreen and Shadmehri, 2003; McKee and Tan, 2003) suggests that conditions during cluster formation may favor the formation of protostellar cores characterized by higher turbulent speeds, higher initial core densities, and as a result, higher time averaged accretion rates during the stellar assembly phase. These conditions, combined with a high number of protostellar cores per unit volume may also produce a larger fraction of more massive stars. Chemical composition – through its affect on protostellar properties – may also play a role in determining both the core accretion rates and emerging IMF.

Direct observations of rich, dense clusters should in principle enable determination of (1) the shape of the initial mass function over the entire range of masses, from $\sim 100 M_{\text{sun}}$ to well below 1 M_{sun} ; (2) the time-averaged accretion rates characteristic of protostellar cores through direct observation of the ‘stellar birthline’ in very young clusters; and (3) the relationship between emerging stellar masses and local stellar density within a given cluster - a potential measure of the importance of collisions between protostellar cores and mergers in forming high mass stars.

Familiar examples of nearby rich, dense clusters are (1) the Arches Cluster located near the center of the Milky Way galaxy; and (2) R136 in the Large Magellanic Cloud. Attempts to carry out detailed studies of these regions with current facilities have thus far been limited primarily by crowding – which limits the accuracy of photometric probes of luminosity functions diagnostic of $N(M)$ and the location of the birthline, as well as

precluding spectroscopy of all but the brightest cluster members. The advent of adaptive optics systems on current generation telescopes will advance observations of these nearby regions significantly through their ability to probe crowded regions far more deeply. However, breakthrough observations that enable probes of clusters spanning a wide range of initial density and chemical composition awaits the availability of the exquisite images that can only be provided by telescopes of size 20m and greater owing to the tremendous gain in angular resolution which they will provide.

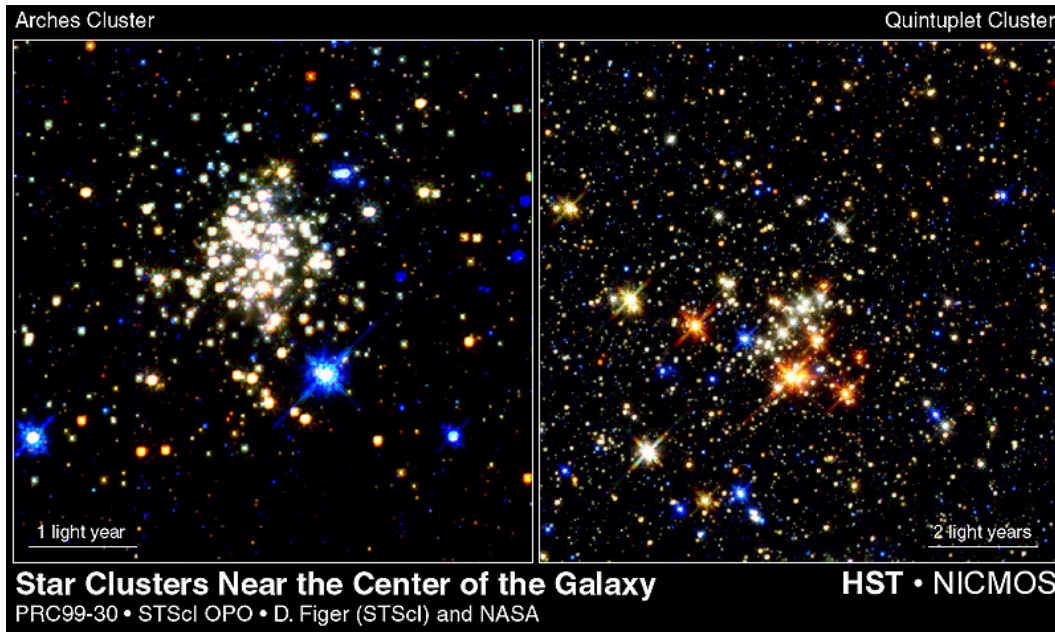


Figure 1. HST NICMOS images of two rich dense clusters near the Galactic Center: Arches (left; see below) and the Quintuplet. The stellar density at the core of the Arches cluster exceeds that of the Orion nebula cluster by at least 10x. The mean distance between stars is < 500 AU in this region.

A Program to Probe Star Formation in Rich, Dense Clusters

Goals

New large (>20 m) telescopes will allow important studies of the initial mass function and the star formation process. The primary gain is in angular resolution which allows for the study of the most dense clusters in local group galaxies and beyond. These clusters are analogs of Milky Way massive clusters like the Arches (Figer et al. 1999), NGC3603 (Brandl et al. 1998), W43 (Blum et al. 1999), W31 (Blum et al. 2001), and others toward the inner Galaxy, as well as R136 (Massey and Hunter 1998) in the LMC. Below, we outline a program for a 30m GSMT equipped with a diffraction limited JHK imager and compatible IFU which will allow study of the IMF over a range of metallicity, cluster density, and galactic environment. The target clusters will also provide a sample with

which to study the effect of the same parameters on the star formation process, or more specifically the location of the stellar birth line for the low mass stars still descending onto the main sequence.

We develop the technical justification for this science case using the known properties of young massive clusters in the Milky Way galaxy and the LMC. Based on the recent work of Hillenbrand and Carpenter (2000, hereafter HC00), we outline a set set of observations which will probe both the high and low mass end of the IMF in a variety of environments.

HC00 presented a new method to statistically estimate the IMF in the Orion Trapezium cluster, paying particular attention to the low mass end ($3 < M_{\text{sun}} < 0.02$). We propose to apply this method in general. The HC00 method seeks to take an infrared color magnitude diagram and deduce a mass function from it. The reader is referred to their paper for details, but briefly the method can be described as follows. Given an infrared color magnitude diagram (CMD; e.g., H-K vs. K), one seeks to find a statistical estimate for the mass function, taking into account the observational uncertainties, a distribution of stellar ages, a distribution of intrinsic excesses (due to accretion disk emission), and a distribution of line of sight extinction. Each of these parameters effects the color and magnitude of a star in the CMD. Since the observed colors are degenerate to different combinations of these parameters, the method seeks to find the most probable mass for any point in the CMD given that the excess, extinction, and age have statistical distributions which can some how be determined independently or reliably assumed.

Once the distributions are in hand, an appropriate set of stellar models is then used to find the most probable mass for any star (or localized group of stars) in the CMD. In the following, we describe the necessary data sets needed to obtain these distributions, and the IMFs in star clusters in and beyond the Milky Way.

These data will not only allow for an unprecedented investigation of the IMF which is critical to star formation history calculations in the early universe, but also for a new exploration of aspects of the star formation process in massive clusters. What is the spatial distribution of the more massive stars relative to the lower mass stars? If massive stars preferentially form in the densest parts of clusters, this implies collisions or mergers could play a role in their formation. Do the most massive stars form in the most dense clusters? With deep imaging in a range of stellar environments including the Milky Way, and Magellanic Clouds, we hope to explore the location of the stellar birthline for low mass stars (Palla and Stahler, 1990) (Figure 2). This locus in the Hertzsprung--Russell Diagram (HRD) may be a function of cluster density or metallicity since it depends on the mass accretion rate.

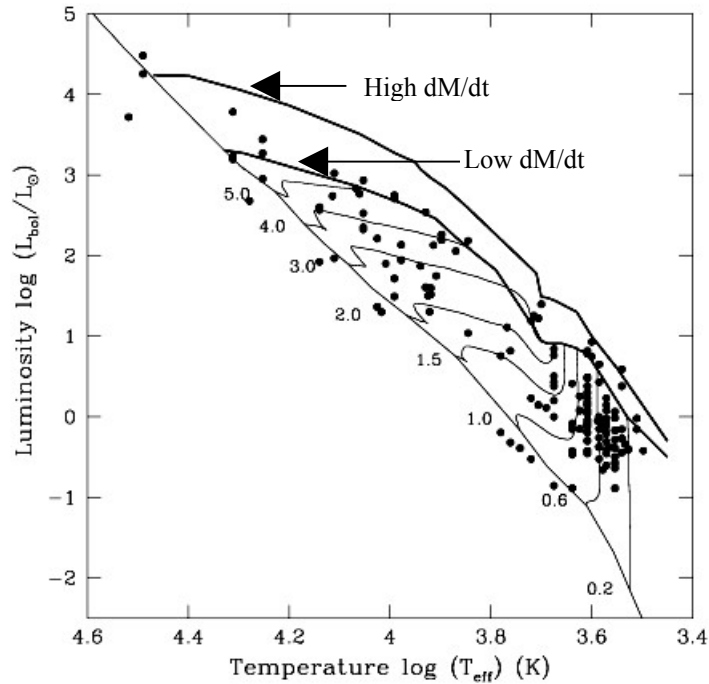


Figure 2. Hertzsprung-Russell Diagram for young star forming clusters (from Paller and Stahler 1990). The effect of higher time-averaged accretion rate during the stellar assembly phase is to raise the birth line in the HRD. The location of post birthline PMS tracks for masses spanning the range from 0.2 to 5 solar masses.

Required Measurements

(a) Deep Infrared Imaging

The basic data needed for this program are deep near infrared images in H and K taken with a near diffraction limited GSMT. We have carried out calculations to determine the photometric limits for Arches or R136 like clusters from the LMC to M82. The intrinsic cluster properties are shown in Table 1. Imaging in Galactic clusters is also crucial, but this work can be done to well below a solar mass on current 8m telescopes with adaptive optics. Determining the distributions of age, excess, and extinction to individual stars will, however, need to be carried out in Galactic clusters with GSMT spectroscopy (see below).

We have computed photometric crowding and photon statistic limits for target environments in the LMC, M33, and M82 using the cluster properties in Table 1 and the crowding limit algorithm given by Olsen et al. (2003). The input luminosity function used for these calculations is a hybrid based on measurements in the Arches cluster (Blum et al. 2002) for the high mass stars ($\sim > 2 M_{\text{sun}}$) and measurements in the Trapezium by HC00 for the low mass stars ($\sim < 3 M_{\text{sun}}$); see Figure 3. The Arches radial profile is a fit to a re-analysis of the Figer et al. (1999) HST data by Blum et al. (2002), while the profile for R136 is taken from Mackey and Gilmore (2003).

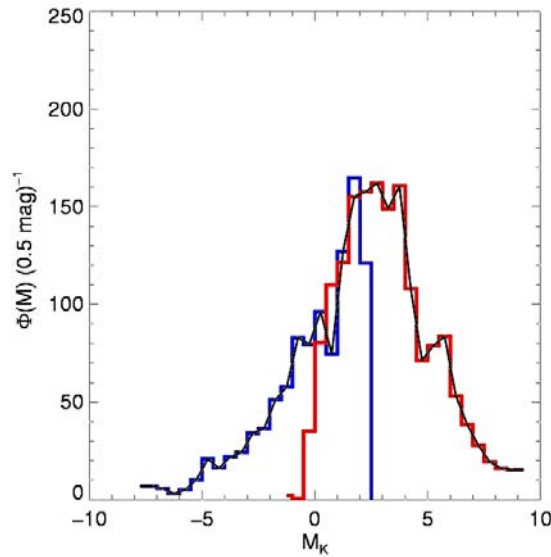


Figure 3. Hybrid K-band luminosity function adopted for the crowding calculations reported herein. The upper end ($M > \sim 2 M_{\text{sun}}$) is adopted from the Blum et al. (2002) analysis of Gemini adaptive optics observations of the Arches cluster. The resulting mass function is slightly steeper than the mass function of Figer et al. (1999) and Stolte et al. (2001). The power law fit gives $\Gamma = -1$, compared to $\Gamma = -1.35$ for a Salpeter (1955) mass function. The low mass end of the mass function is taken from HC00.

Table 2 lists the results of these calculations for 8m, 20m, 30m, 50m, and 100m telescopes which have diffraction limited PSF at 2.2 microns of 0.0563", 0.0225", 0.0150", 0.0090", and 0.0045", respectively. The last two cases were considered in order to provide a comparison to the expected performance of the Euro50 (50m) and ESO OWL (100m) telescopes. The tables show the detailed results for Arches-like clusters. The cases for the Arches and R136 are graphically summarized in Figure 4 for two particular surface brightnesses (Table 1). The immense performance increase over current ground based telescopes for the GSMT (and larger) telescopes is clearly evident. Incredibly, the observations are no longer crowding limited in M33 for a 100m telescope! Photon limited accuracy of 10% would require the exposure times listed in Table 2.

Table 1. Massive Star Cluster Properties
Cluster Surface Brightness (K mag/sq arcsec)

R_e	Arches	R136
0.5	10.5	13.3
1	11.9	14.8
2	13.6	16.5
5	16.2	18.9

Note to Table 1- For Arches, we assume a scale radius, $a = 0.27$ pc, a radial profile of the form surface brightness $\sim (1 + r/a)^3$, and a half light radius, $R_e = 0.6$ pc. The corresponding quantities for R 136 are 0.36 pc; $1/(1+r^2/a^2)^\gamma$, with $\gamma = 2.4$; and 1.1 pc.

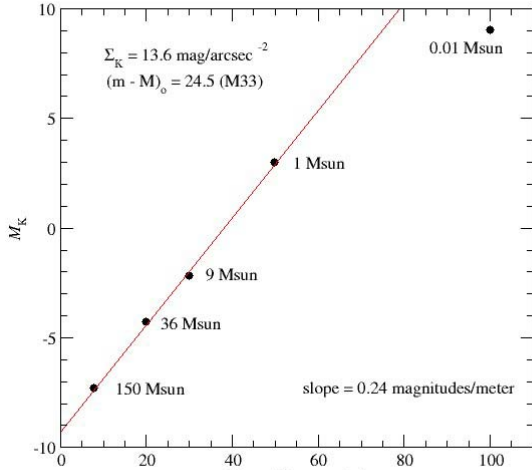


Figure 4a. Limiting absolute K magnitude as a function of telescope diameter for Arches like clusters. For the KLF chosen here, the 30m GSMT will resolve individual stars with masses less than 10 Msun in young, starburst like clusters at the distance of M33! The surface brightness is appropriate to a radius containing 1/2 the cluster luminosity.

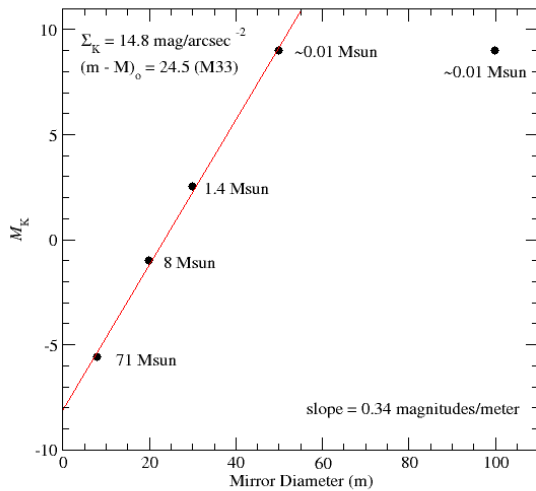


Figure 4b. Same as 3a, but for the R136 case. R136 is a factor of 10 less dense than the Arches (Figer et al. 1999), and even lower mass objects would be detected at the distance of M33. As above, the surface brightness is appropriate to a radius containing 1/2 the cluster luminosity.

Table 2a: Crowding and Corresponding Lower Mass Limits (100m GSMT)

Radius (R _c)	Limiting K-magnitude			Limiting Mass			Exposure Time		
	LMC	M33	M82	LMC	M33	M82	LMC	M33	M82
0.5	>27.5	15.5	<19.8	~0.01	20	>200	100	<0.01	<0.01
1	>27.5	26.5	19.8	~0.01	1.8	200	100	17	<0.01
2.0	>27.5	>33.5		~0.01	~0.01			10000 @	
5.0	>27.5	>33.5	>36.8	~0.01	~0.01	~0.01	100	K=30	2

Table 2b: Crowding and Corresponding Lower Mass Limits (50m GSMT)

Radius (R _c)	Limiting K-magnitude			Limiting Mass			Exposure Time		
	LMC	M33	M82	LMC	M33	M82	LMC	M33	M82
0.5	>27.5	18.5	<19.8	~0.01	78	>200	1500	<0.01	<0.01
1.0	>27.5	21.5	<19.8	~0.01	20	>200	1500	0.1	<0.01
2.0	>27.5	27.5	21.7	~0.01	1.1	80	1500	1500	0.1
5.0	>27.5	>33.5	26.8	~0.01	~0.01	7.6	1500	10000	@K=28.5

Table 2c: Crowding and Corresponding Lower Mass Limits (30m GSMT)

Radius (R _c)	Limiting K-magnitude			Limiting Mass			Exposure Time		
	LMC	M33	M82	LMC	M33	M82	LMC	M33	M82
0.5	>27.5	17	<19.8	~0.01	170	>200	12000	0.0	0.03
1.0	>27.5	18.9	<19.8	~0.01	65	>200	12000	0.01	0.03
2.0	>27.5	22.3	20	~0.01	3	193	12000	1.5	0.04
5.0	>27.5	27.5	23.9	~0.01	1.1	32	12000	12000	25

Table 2d: Crowding and Corresponding Lower Mass Limits (20m GSMT)

Radius (R _c)	Limiting K-magnitude			Limiting Mass			Exposure Time		
	LMC	M33	M82	LMC	M33	M82	LMC	M33	M82
0.5	26.6	<16.5	<19.8	0.1	>200	>200	10000	<0.01	<0.1
1.0	26.6	17.6	<19.8	0.1	135	>200	10000	<0.01	<0.1
2.0	26.6	20.2	<19.8	0.1	36	>200	10000	0.1	<0.1
5.0	26.6	26.6	22.2	0.1	1.8	69	10000	10000	5

Table 2e: Crowding and Corresponding Lower Mass Limits (8m)

Radius (R_c)	Limiting K-magnitude			Limiting Mass			Exposure Time		
	LMC	M33	M82	LMC	M33	M82	LMC	M33	M82
0.5	16.3	<16.5	<19.8	13	>200	>200	0.01	0.01	<3
1.0	24.6	<16.5	<19.8	0.25	>200	>200	10000	0.01	<3
2.0	24.6	17.2	<19.8	0.25	150	>200	10000	0.03	<3
5.0	24.6	21.5	<19.8	0.25	20	>200	10000	40	<3

Notes to Table 2- The distance moduli used for the calculations were 18.5, 24.5, and 27.8 for the LMC, M33, and M82, respectively. *K*-band magnitudes are for crowding limited photometry to 10% accuracy. Mass to *K* magnitude transformation as given in Blum et al. (2002).

(b) Spectra

While the final HC00 analysis is based on photometric data, the method relies on large numbers of individual spectra in order to produce the distributions of age and excess emission for a given cluster. These properties are derived from the spectral types of the individual stars. Ideally, the spectra would sample the entire range of colors and magnitudes in the (H-K vs. K) CMD. Ages, individual excesses, and extinctions would be produced and the frequency distribution of each would be applied to the CMD when inverse mapping each location in the CMD from color and magnitude to mass.

HC00 applied the spectroscopically derived distributions uniformly to their photometric data which covered a relatively narrow range of masses. In the present case, different distributions may be applied to different magnitude bins. For example, it may be expected that the distribution of intrinsic excess will be different for high and low mass stars.

For more distant clusters, we will need to assume the distributions of excess emission and age for stars in the CMD which are too faint to be observed spectroscopically. Appropriate distributions can be derived (extrapolated) from the Galactic and LMC clusters which are more nearby and sample a range of metallicities and densities.

Based on the analysis of HC00, the mass function results appear to be robust even for relatively large uncertainties in the excess and age distributions. Assuming the distributions will be broadly similar in the massive clusters we observe, then one to two hundred stars with good quality spectra (S/N 100 - 50, where hotter, more luminous stars need higher S/N due to weaker features) will be sufficient.

HC00 used optical colors and spectra to derive the extinction to and ages of individual stars. With appropriate colors corresponding to each, they used the observed H - K to derive the excess emission to each star. We will generally not have optical data to work with, and will thus iteratively determine the extinction and intrinsic excess using the infrared spectra obtained with the GSMT. For the hot stars, the colors will be dominated by extinction (reddening) except for a few high mass objects still enshrouded in their birth material (e.g., W31, Blum et al. 2001). For the low mass stars, accurate spectral type

classifications exist which will allow for the extinction and excess to be determined iteratively from the near infrared colors and spectra (See, e.g., Ali et al. 1997).

Table 3. Exposure Times for R = 1000 Spectroscopy with a 30m Telescope

Stellar Parameters		LMC		M33		M82	
M_K	Mass (M_{sun})	K	t_{exp} (sec)	K	t_{exp} (sec)	K	t_{exp} (sec)
-7.75	192	10.75	1	16.75	30	20.0	964
-6.75	119	11.75	1	17.75	77	21.0	3960
-5.75	74	12.75	1	18.75	214	22.0	19000
-4.75	46	13.75	2	19.75	663	23.0	
-3.75	28	14.75	5	20.75	2520	24.0	
-2.75	17	15.75	12	21.75	12000	25.0	
-1.75	11	16.75	30	22.75	63000	26.0	
-0.75	6.7	17.75	77	23.75		27.0	
0.25	4.2	18.75	214	24.75		28.0	
1.25	2.6	19.75	663	25.75		29.0	
2.25	1.6	20.75	2520	26.75		30.0	
3.25	0.99	21.75	12000	27.75		31.0	
4.25	0.61	22.75	63000	28.75		32.0	

In Table 3, we tabulate the exposure times required to reach S/N 50 for the cluster stars as a function of K magnitude. The exposure times were calculated with an exposure time calculator (ITC) developed by Gregory (2003) for the GSMT. We assume a near-IR IFU spectrograph; a 0.015" slit; and resolving power $R = 1000$. We note that stars with $K < 17$ can be observed with current generation telescopes. For embedded Milky Way clusters, the exposure times will be similar to those in the LMC owing to the compensating effects of extinction and distance. However, in such clusters, extinction dominates, and we will not be able to observe objects to as low a mass as in the LMC.

Using the results of Table 3, we can estimate the total time to survey Galactic, LMC, and extra galactic clusters. Assuming a diffraction limited IFU spectrograph with M deployable IFUs, each with a FOV of roughly 0.5" x 0.5" for which the multiplex gain is m stars, then our program would take a total time $T = 420 \text{ hr} * N \text{ clusters} / (m * M) / (100 \text{ cluster stars})$. Taking $m=2$, $M=10$, this is 21 hrs per cluster. To observe 10 clusters would thus take about 200 hr.

References

Ali, B., Sellgren, K., Depoy, D.L., Carr, J.S., Gatley, I., Merrill, K.M., & Lada, E. 1998, ASP Conf. Ser. 154: Cool Stars, Stellar Systems, and the Sun, 10, 1663

Blum, R. D., Daminieli, A., & Conti, P. S. 1999, AJ, 117, 1392.

Blum, R. D., Conti, P. S., & Daminieli, A. 2001, AJ, 121, 3149

Blum, R.~D., Conti, P.~S., Daminieli, A., & Figueredo, E. 2002, Hot Star Workshop III: The Earliest Stages of Massive Star Birth. ASP Conference Proceedings, Vol. 267. Edited by Paul A. Crowther. ISBN: 1-58381-107-9. San Francisco, Astronomical Society of the Pacific, 2002, p.283

Brandl, B., Brandner, W., Eisenhauer, F., Moffat, A.F.J., Palla, F., & Zinnecker, H. 1999, A&A, 352, L69

Elmegreen, B.G. and Shadmehri, M. 2003, M.N.R.A.S. 338, 817.

Figer, D. F., Kim, S. S., Morris, M., Serabyn, E., Rich, R. M., & McLean, I. S. 1999, ApJ, 525, 750

Gregory, B. & Zenteno, A. 2003, see
<http://www.noao.edu/noao/staff/brooke/gsm/gsm.php>

Hillenbrand, L. & Carpenter, J. 2000, ApJ, 540, 236

Mackey, A., Gilmore, G. 2003, MNRAS, 385, 85

Massey, P. & Hunter, D. A. 1998, ApJ, 493, 180

McKee, C. and Tan, J. 2003, ApJ, 585, 850

Olsen, K., Blum, R.D., & Riguat, F. 2003, AJ, 126,

Palla, F. and Stahler, S. 1990, ApJ 360, 47

Salpeter, E. E. 1955, ApJ, 121, 161